# **ENVIRONMENTAL RESEARCH**

**LETTERS** 



#### **OPEN ACCESS**

#### RECEIVED

2 May 2024

#### REVISED

8 October 2024

ACCEPTED FOR PUBLICATION 17 October 2024

PUBLISHED

29 October 2024

Original content from this work may be used under the terms of the Creative Commons Attribution 4.0 licence.

Any further distribution of this work must maintain attribution to the author(s) and the title of the work, journal citation and DOI.



#### **LETTER**

# Leveraging synthetic aperture radar (SAR) with the National Water Model (NWM) to improve above-normal flow prediction in ungauged basins

Shiqi Fang<sup>1,\*</sup>, J Michael Johnson<sup>2</sup> and A Sankarasubramanian lo

- Department of Civil, Construction and Environmental Engineering, North Carolina State University, Raleigh, NC, United States of America
- <sup>2</sup> Lynker, Fort Collins, CO, United States of America
- \* Author to whom any correspondence should be addressed.

E-mail: sfang6@ncsu.edu

Keywords: synthetic aperture radar, predictions, ungauged, streamflow

Supplementary material for this article is available online

#### **Abstract**

Effective flood prediction supports developing proactive risk management strategies, but its application in ungauged basins faces tremendous challenges due to limited/no streamflow record. This study investigates the potential for integrating streamflow derived from synthetic aperture radar (SAR) data and U.S. National Water Model (NWM) reanalysis estimates to develop improved predictions of above-normal flow (ANF) over the coterminous US. Leveraging the SAR data from the Global Flood Detection System to estimate the antecedent conditions using principal component regression, we apply the spatial-temporal hierarchical model (STHM) using NWM outputs for improving ANF prediction. Our evaluation shows promising results with the integrated model, STHM-SAR, significantly improving NWE, especially in 60% of the sites in the coastal region. Spatial and temporal validations underscore the model's robustness, with SAR data contributing to explained variance by 24% on average. This approach not only improves NWM prediction, but also uniquely combines existing remote sensing data with national-scale predictions, showcasing its potential to improve hydrological modeling, particularly in regions with limited stream gauges.

## 1. Introduction

Developing accurate flood prediction models provides critical information to ensure sustainable flood risk management, early warning systems, and lifesaving responses (Maidment 2009, Johnson et al 2016). In the United States, the NOAA Office of Water Prediction provides streamflow forecasts for the entire river network of the United States (National Weather Service 2022, Salas et al 2023) through the National Water Model (NWM). The NWM forecasts are used to generate flood inundation maps (Johnson et al 2019) which are being used by River Forecasting Centers to provide operational guidance during flood events. However, the operational skill can still benefit from improved above-normal flows (ANF) (defined as exceeding the 67th percentile flow) as the raw NWM outputs suffer from both

marginal and conditional biases (Johnson *et al* 2023). Developing postprocessing models have been shown to enhance the NWM forecast skill, however, NSEs of forecasts for ANF conditions near gauged locations are only skilled in 50% of evaluated basins (Frame *et al* 2021, Johnson *et al* 2023, Fang *et al* 2024). The ability to predict ANFs is likely worse in ungauged basins, particularly in regions with limited USGS gauging stations, highlighting the need for improved ANF prediction using NWM forecasts.

Recent advancements in remote sensing (RS) data have emerged as a viable alternative to supplement *in situ* observations and process-based models (Xu *et al* 2021, Sogno *et al* 2022, Tayal *et al* 2024). Studies show they can benefit real-time forecasting capabilities, particularly in estimating the current stage and discharge (Van Dijk *et al* 2015). RS data have been an important component of the Global Flood Monitor

System (GFMS), which has been running in real-time for the last few years with data products (including rainfall, flood, and Tropical Cyclone) being displayed at the NASA tropical rainfall measuring mission (TRMM) website (http://trmm.gsfc.nasa.gov/). The GFMS uses satellite-based estimates of precipitation to estimate runoff generation, routing, and flood inundation attributes such as stage. However, the challenge is effectively translating RS data into accurate streamflow forecasts in ungauged basins as it only provides antecedent conditions with limited information on future flood potential.

Streamflow forecasts are typically developed using process-based models (Wood et al 2011, Archfield et al 2015, Clark et al 2015) and/or datadriven models (Kratzert et al 2019). Traditionally process-based models have been used to tackle the 'grand challenge of hydrology' of achieving consistence hydrologic prediction everywhere on earth (Wood et al 2011, Sperna Weiland et al 2012). And while efforts have substantially improved these modeling paradigms, successfully achieving accurate hydrologic prediction everywhere remains a challenge due to difficulties in estimating antecedent conditions particularly in regions with limited stream gauges. Process-based models can utilize remotely derived variables like precipitation, soil moisture, and evapotranspiration (Vinukollu et al 2011, AghaKouchak et al 2015). To this end, there are numerous studies focused on incorporating synthetic, in situ, or RS-derived antecedent conditions into forecasting systems (Mazrooei and Sankarasubrama 2019, Mazrooei et al 2021). For example, Revilla-Romero et al (2016) utilized the ensemble Kalman filter to integrate low-resolution satellite-based flood extents from the Global Flood Detection System (GFDS) into a global forecasting system aimed at real-time flood forecasting. The forecast developed using remotely sensed data such as GFDS data ignores the potential changes in the precipitation and temperature in the upcoming days/weeks.

While streamflow can be derived from RS instruments, e.g. MODIS (Tarpanelli et al 2019, Sahoo et al 2022) or LANDSAT (Gleason et al 2014), these sensors provide lower spatial resolution and can be impeded by clouds and other obstacles—particularly in periods of above-normal or high flows (Alquraish and Khadr 2021). On the other hand, technologies such as synthetic aperture radar (SAR) can provide high-resolution images of water conditions, even in adverse weather conditions (Tsokas et al 2022, Yoon et al 2022). Streamflow estimation using SAR data usually involves building empirical relationships between ground-measured streamflow and the SAR data to estimate above-normal/high flow signal (Yoon et al 2022); a curve number approach by estimating runoff from rainfall amounts (Hong and Adler 2008, Beck et al 2009); or a histogram thresholding

or clustering method to separate flooded from nonflooded areas in SAR imagery (Martinis et al 2009). Hostache et al (2018) employed a modified particle filter with sequential importance sampling to integrate probabilistic flood maps from SAR into a hydrologic and hydraulic model, while Cooper et al (2018) demonstrated that assimilating SAR backscatter could outperform transforming it into water levels. While the mentioned studies have demonstrated notable skill in predicting streamflow at a basin scale, their applicability on a continental scale (e.g. Coterminous US) has not been demonstrated to date. Further, assimilating RS data into a processbased hydrological models at continental scales typically requires heavy computational demand. Under these situations, data-driven methods like spatiotemporal hierarchical model (STHM) (Fang et al 2024) or long short-term memory (Feng et al 2020, Frame et al 2021), can provide a hybrid approach that leverage RS products and physics-based model outputs to develop ABN predictions at continental scale. Recently, Fang et al (2024) introduced a STHM model that improved NWM streamflow predictions using a set of catchments and hydroclimatic characteristics and antecedent conditions estimated based on three-day averaged streamflow observations available within the Hydrologic Unit Code (HUC)-8. While this study presented a post-processing model that improved ANF prediction across the coterminous US (CONUS) basins, but the approach had limited skill in predicting ANF for coastal basins and in obtaining antecedent streamflow conditions particularly in regions with limited stream gauge stations (e.g. several HUC8s in Region 09 Souris-Red-Rainy basin or Region 13 Rio Grande).

The aim of this study is to understand if the process based NWM, a suite of hydroclimate and basin characteristics, and SAR streamflow data can be integrated to improve on previous STHM efforts to provide improved ANF estimates. The paper is structured as follows: section 2 outlines the materials and data used, section 3 presents the results with a thorough analysis of the model's predictions, and section 4 discusses the results, emphasizing research gaps and suggesting potential solutions to overcome challenges.

## 2. Materials and methods

# 2.1. NWM Predictions, Hydroclimate and land use data

The NWM makes predictions across a modified version of the National Hydrographic Dataset (NHDPlusV2, McKay *et al* 2012, Blodgett *et al* 2023). The NWM is a continental-scale distributed high-resolution hydrologic model that produces streamflow predictions for 2.7 million stream reaches across

the CONUS, based on a variety of data ranging from radar-gauge observed precipitation to numerical weather prediction (National Research Council 2006). The NWM relies on the Weather Research and Forecasting hydrologic model architecture (Ghotbi et al 2020) and provides streamflow predictions extending up to 30 d in advance over the CONUS. NWM provides these predictions at gauged locations but still consists of errors, which depend on both hydrologic process representation and forcing errors (Viterbo et al 2020). To compare forecasts to observations, co-located common feature IDs and USGS National Water Information System gauges were extracted from the Routelink file associated with NWM v2.1. Catchment characteristics were accessed from Johnson et al (2023) and Fang et al (2024) which summarized hydroclimatic, land use, and anthropogenic characteristics (e.g, upstream storage) to gage locations in the Gages II Network (Falcone 2011). Furthermore, the GAGESII dataset includes the 2009 hydro-climatic network categories, distinguishing between controlled and natural basins. Lastly, the REACHCODE associated with the NHDPlusV2 COMID enables the identification of Hydrologic Unit Code (HUC) regions provided by the Watershed Boundary Dataset. All the abovementioned data can be accessed at https://github. com/LynkerIntel/nwm-evaluation-2023.

# 2.2. Water surface metrics from GFDS-SAR

The GFDS provides a flood monitoring system created by the Joint Research Centre of the European Commission in partnership with the Dartmouth Flood Observatory at Colorado University (www.gdacs.org/flooddetection/Download/ Technical\_Note\_GFDS\_Data\_Products\_v1.pdf).

The system integrates satellite measurements from sensors including the TRMM, Global Precipitation Measurement Mission, Advanced Microwave Scanning Radiometer-Earth, and AMSR2. These measurements are amalgamated to generate a variety of products displaying flood signals. GFDS water surface metrics have been instrumental in numerous studies (Van Dijk *et al* 2016, Yoon *et al* 2022). Moreover, various real-time flood monitoring applications rely on the data streams provided by GFDS.

GFDS estimates water surface metrics using brightness temperatures. If the physical temperature remains constant, changes in brightness can be assumed to be caused by changes in water in the pixel. Since the raw values are influenced by factors such as physical temperature, permittivity, surface roughness, vegetation, atmospheric moisture, and other environmental variables (Kugler and De Groeve 2007, Van Dijk *et al* 2016),  $T_{\rm b,measurement}$  refers to the measured brightness temperature during wet conditions. An M/C value can be defined as the ratio of measurement ( $T_{\rm b,measurement}$ ) /wet signal ( $T_{\rm b,calibration}$ )

over calibration/dry observations, which is detected by SAR as water surface signal for proxy streamflow:

$$S = \frac{M}{C} = \frac{T_{\text{b,measurement}}}{T_{\text{b,calibration}}} \tag{1}$$

where, T<sub>b</sub> is passive microwave radiometers, brightness temperature, subscript 'measurement' and 'calibration' *M* and *C*, respectively. These can be accessed from GFDS website (www.gdacs.org/flooddetection/DATA/SINGLE/SignalTiffs/). We use *M/C* ratio, which provides a measure of how the brightness temperature (representing surface water or wetness) in a given area deviates from normal dry conditions, which can then be used to infer streamflow or flood conditions. Once the river stage is sensed based on the *M/C* value, we use that to assess the antecedent conditions of the river.

# 2.3. Principal component regression (PCR) of M/C ratio

Since the M/C ratio provided by GFSD is spatially explicit and correlated, we use principal component analysis (PCA) to reduce the dimension to estimate the conditions of a given river. PCA helps convert the correlated time series available at multiple grid points into orthogonal components, so that fewer components can explain the observed variance across space. For each gauged location, we retain two components of brightness temperature (T) by performing PCA on the 24 nearest GFDS grid cells and develop a regression with the observed depth of daily streamflow (discharge divided by the drainage area). To perform this, we pool all gauged stations within HUC8 (See figure 1 for detailed steps). Thus, each HUC8 will have a unique regression that can convert the PCs of the M/C ratio available for any given location to estimate the depth of streamflow at ungauged locations.

By utilizing PCA to reduce the dimensionality of the M/C ratio from GFDS data, we effectively capture the essential features of antecedent streamflow conditions for estimating streamflow in ungauged basins. Using the retained two PCs, indexed as 'g', the important features of the antecedent conditions, M/C ratio, have been retained by score matrix ( $T_g$ ) (Camps-Valls and Bruzzone 2005), and then applied a multiple linear regression between  $T_g$  and the observed daily streamflow y, expressed as depth of runoff (i.e. streamflow divided by the drainage area), at gauged stations within the HUC-8:

$$y = T_g C + \epsilon \tag{2}$$

where, the coefficient of regression (*C*) is given by:

$$\hat{C} = \left(T_g^T T_g\right)^{-1} T_g^T y . \tag{3}$$

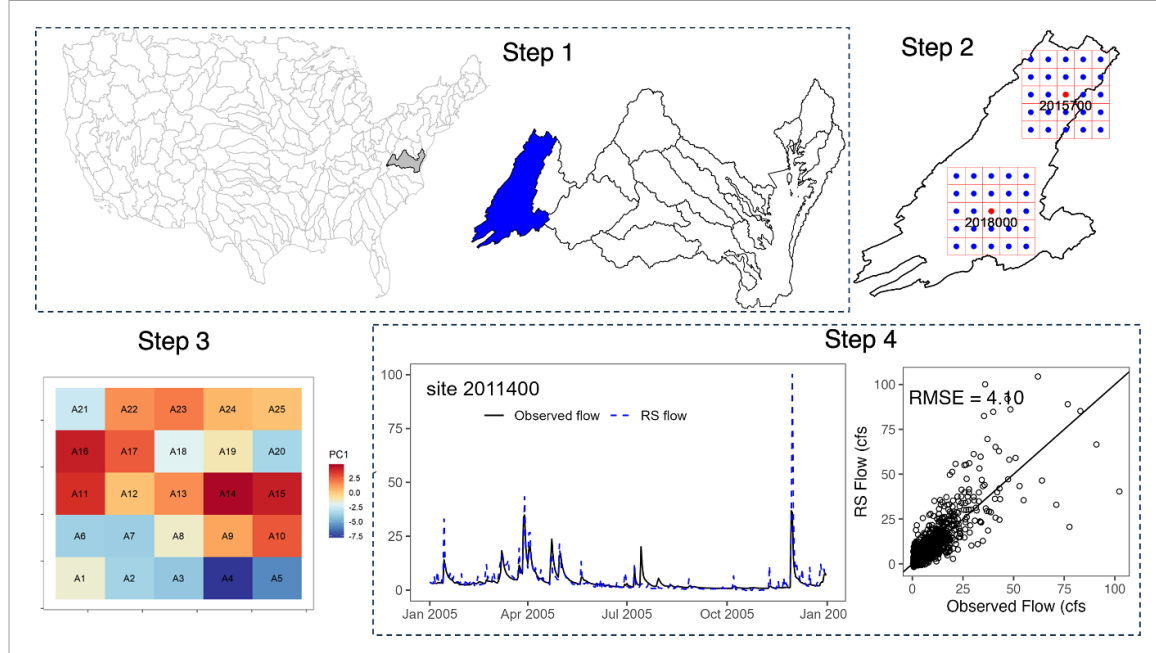


**Figure 1.** Key steps for leveraging SAR data to predict antecedent (i.e. 3 d) streamflow conditions: step 1: identify all Gages-II basins (red dots), grouped within the same HUC8 (colored in blue); step 2: sampling *M/C* data for the gauged locations and the associated 24 neighboring cells; step 3: loadings from the PCA for 24 neighbors; step 4: predicted streamflow based on the multivariate regression (equation (2)) between the first two scores and the observed 3 d streamflow at the selected stations.

# 2.4. STHM for ANF prediction using SAR data (STHM-SAR)

The aim of the study is to use SAR-estimated antecedent streamflow conditions to further advance post processing techniques that can be applied to large scale process-based models. Here, we start with the STHM defined in Fang *et al* (2024) and replace the 3 d area-weighted gaged flows with the SAR-derived streamflow for the previous 3 d. Thus the new SAR informed STHM-SAR can be written as:

$$\begin{split} Q_{\{t(\tau,i,j,k)\}} &= \beta_{\{000,\tau\}} + \beta_{\{1(\tau,i,j,k)\}} Q_{\{t(\tau,i,j,k)\}}^{\text{NVM}} \\ &+ \beta_{\{2(\tau,i,j,k)\}} Q_{\{t(\tau,i,j,k)\}}^{\text{SAR}} \\ &+ \beta_{\{01(\tau,j,k)\}} \text{PET}_{\{\tau(j,k)\}} \\ &+ \beta_{\{001,\tau\}} \text{AI}_{\{i(j,k)\}} + \beta_{\{002,\tau\}} \text{Imp}_{\{i(j,k)\}} \\ &+ \beta_{\{003,\tau\}} \rho_{\{i(j,k)\}} + \varepsilon_{\{t(\tau,i,j,k)\}} \end{split} \tag{4}$$

where,  $Q^{\rm NWM}$  is the NWM daily flow;  $\rho$  is the spearman correlation indicating moisture and energy being in-phase or out-phase; PET is the mean 10 day potential evaporation as mentioned above; AI is the aridity index; Imp is the percent impervious; and  $\varepsilon$  is the residual.

#### 2.5. Model evaluation

To evaluate the skill of our STHM-SAR model, we use the Nash–Sutcliffe efficiency (NSE) (i.e. coefficient of determination,  $R^2$ ) metric which is widely used to measure the predictive skill of hydrological models (McCuen *et al* 2006). The model performance criteria recommended by Moriasi *et al* (2007) was used for evaluating performance meaning predictions were

considered 'acceptable' if NSE scores are greater than 0.5 and 'good' if the NSE is above 0.67.

Since we are interested in assessing the performance of the model for estimating flows in ungauged locations, we use both spatial and temporal validation procedures similar to that of Fang et al (2024). For spatial validation, we used a k(20)-fold crossvalidation method (Browne 2000) treating 5% of locations as ungauged within each hierarchical group and fit the remaining 95% of stations for the period 1993 and 2018. We evaluated the STHM-SAR performance for the period 2009-2018 for the left-out basins. This process of leaving out 5% of the basins is repeated until all evaluated in a cross-validation mode. The temporal validation is performed to evaluate the STHM-SAR performance over a period different from the calibration, whereas the spatial validation is performed to evaluate the STHM-SAR for application in ungauged basins. The temporal validation is performed by calibrating the STHM-SAR model using the data from 1993 to 2008 with the remaining data from 2009 to 2018 being considered for validation. Thus, all the reported model evaluation, NSEs in figures 2-4, are for the period 2009-2018 based on k(20-fold cross-validation.

## 3. Results

We first evaluated the ability of GFDS SAR-derived streamflow (from equation (2) in predicting the observed daily streamflow using spearman rank correlation for all natural basins within the CONUS (figure 2). We also calculated the NSE between

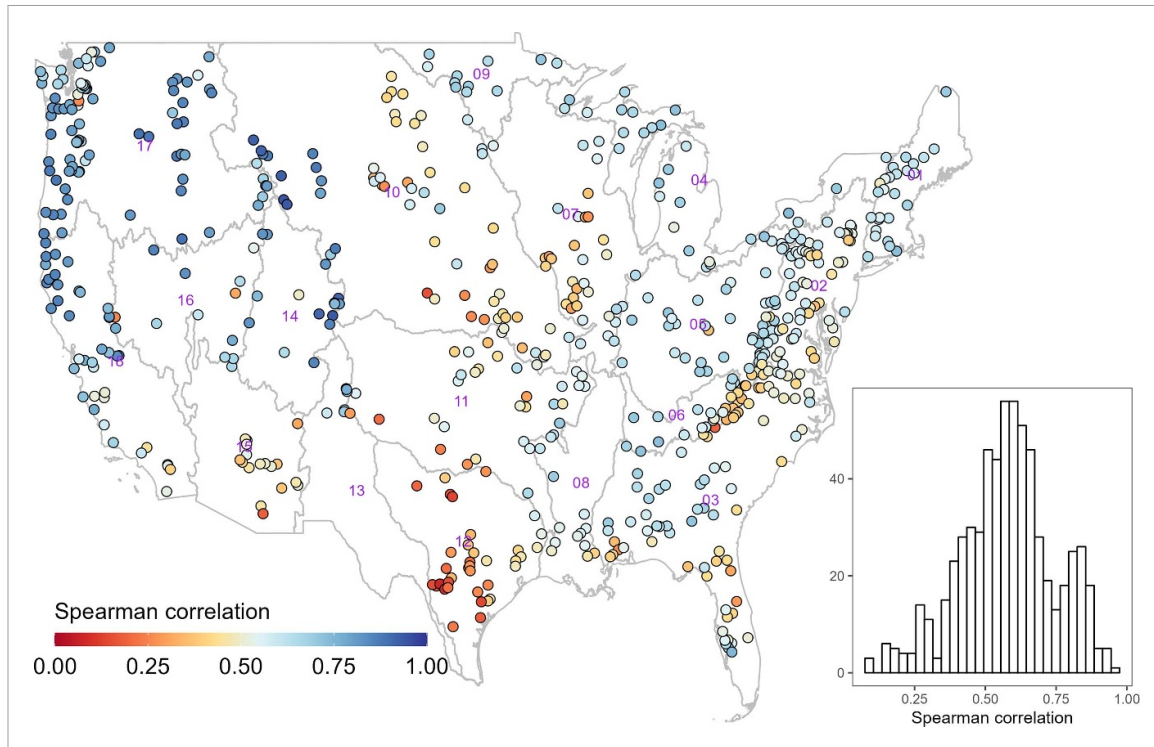


Figure 2. Spearman Rank correlation between above average SAR-derived and observed streamflow (all conditions) for Gages-II basins during the validation period (2010–2018) and the corresponding histogram.

the 3 d average streamflow from the GFDS-SAR and observed 3 d average streamflow (*Y* axis) (figure 3). Figure 3(a) also compares the NSE from the GFDS-SAR with the NSE (*X*-axis) between the 3 d average streamflow estimated based on the simple depth of streamflow using the drainage area method (i.e. without using the GFDS-SAR stage estimates) with the observed streamflow. We then conducted an analysis of model performance using SAR-derived data (figure 4) and present an examination of contributing factors in the STHM-SAR compared to the base STHM (Fang *et al* 2024).

# 3.1. Performance of SAR-derived streamflow in estimating observed streamflow

The correlation between SAR-derived and observed streamflow varies across the CONUS (figure 2). Figure 2 shows improvement in estimating 3 d streamflow using the SAR-derived streamflow when compared with the 3 d streamflow estimated using the drainage area method The correlation between SAR-derived streamflow and observed above average streamflow is notably strong, as depicted in figure 2. Across all Gages-II basins, the mean correlation exceeded 0.53 for high flows during validation, underscoring the reliability of the SAR-derived streamflow in estimating the antecedent conditions. Spatially, the Northwest region exhibited the highest correlation, while the lowest correlation was observed around the 95th meridian (Seager and Ting 2017, Johnson et al 2023). Notably, the Tennessee River

Basins demonstrated limited performance by using SAR-derived high streamflow. One potential reason could be due to steep terrain and heavily controlled flows due to the reservoir cascade is perhaps limiting the ability to predict ABN flows. Prior work from Van Dijk *et al* (2016) suggested that the most successful in natural basins (with R > 0.8) are concentrated in the southeast of the USA. However, their focus was on the entire daily streamflow time series whereas we focus primarily in estimating high flows in figure 2.

Comparing the  $R^2$  values between GFDS SARderived streamflow and the 3 d average streamflow with the  $R^2$  values obtained using the simple drainage-area method (as performed in Fang et al 2024) shows that GFDS-SAR derived streamflow consistently performs better than the drainage-area method in explaining the variability observed 3 d streamflow (see figure 3(a)). Moreover, figure 3(b) shows that the improved performance of SAR derived streamflow decreased as the number of gauges increases in the same HUC08. This underscores that these performance enhancements are notably more significant in basins with limited streamflow gauges, which is 29% of basins, mostly coastal basins, that have less than 2 gauges within a HUC8 (<150 km along coastal line, Fang et al 2024). Previous studies (Frame et al 2021, Johnson et al 2023) also show challenges in estimating streamflow for basins with limited gauges particularly in the coastal areas and Missouri basin. Thus, this improvement is critical that can help in the better estimation of antecedent

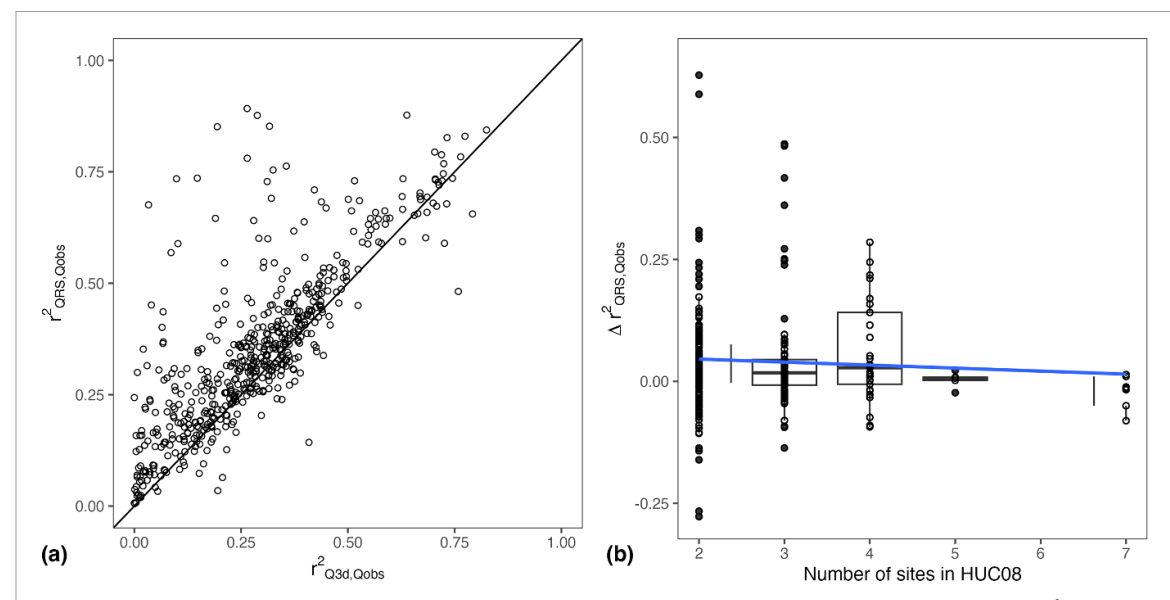
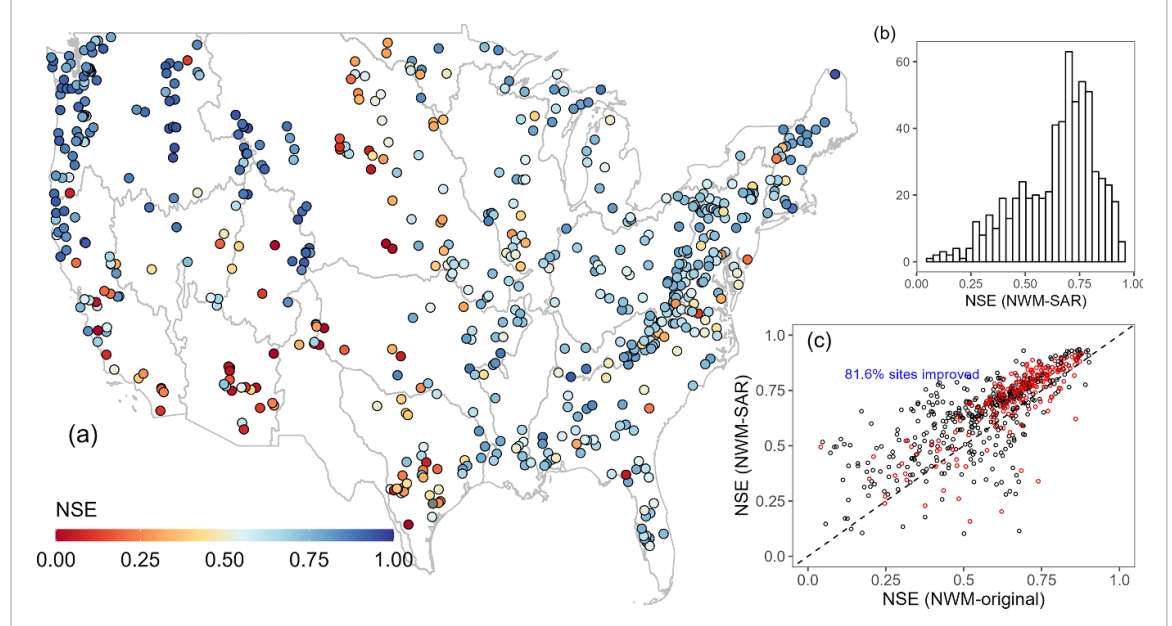


Figure 3. Improvements in predicting 3 d streamflow using SAR data and PCR (equation (2)) for natural basins. Left:  $r^2$  between the SAR-derived 3 d streamflow (Y axis) and observed 3 d streamflow compared with the  $r^2$  between the 3 d streamflow estimated using the drainage area (X-Axis) (Fang et al 2024) and the observed 3 d streamflow. Right: SAR-derived streamflow r-squared values improvements ( $\Delta r^2$ ) from previous 3 d streamflow relationship as a function of number of sites within the same HUC08.



**Figure 4.** Performance evaluation of STHM-SAR in improving ABF predictions for natural basins during cross-validation: (a) spatial distribution of NSE from the STHM-SAR model in predicting ABF conditions (>67%),(b) histogram of NSE from the STHM-SAR model, (c) comparison of NSE from the STHM-SAR model with the NSE of the raw NWM outputs, red points are costal site within 150 km from the coastline (Fang *et al* 2024).

conditions particularly in coastal basins and regions with limited streamflow gauges.

# 3.2. STHM-SAR improves above-normal streamflow predictions

Next, we look more closely at how the STHM-SAR enhances NWM predictions in ANF events obtained based on k-20 cross validation (as illustrated in figure 4). From figure 4(b), we infer 81.6% of the sites exhibit improved skill compared to the NWM alone. Most of these improved sites were concentrated

in HUC2 regions (01–06, 15–18 as shown in figure 2). The most substantial enhancements were observed in the northwest regions, where over 85% of the sites exhibited NSE values greater then 0.67. In comparison with the findings of the gage aggregated STHM from (Fang *et al* 2024), the STHM-SAR demonstrated notable improvements, particularly in coastal sites, showcasing an average NSE improvement of 0.15. This highlights the benefits of estimating antecedent conditions using SAR data to better predict highflow events. The accuracy of streamflow forecasting

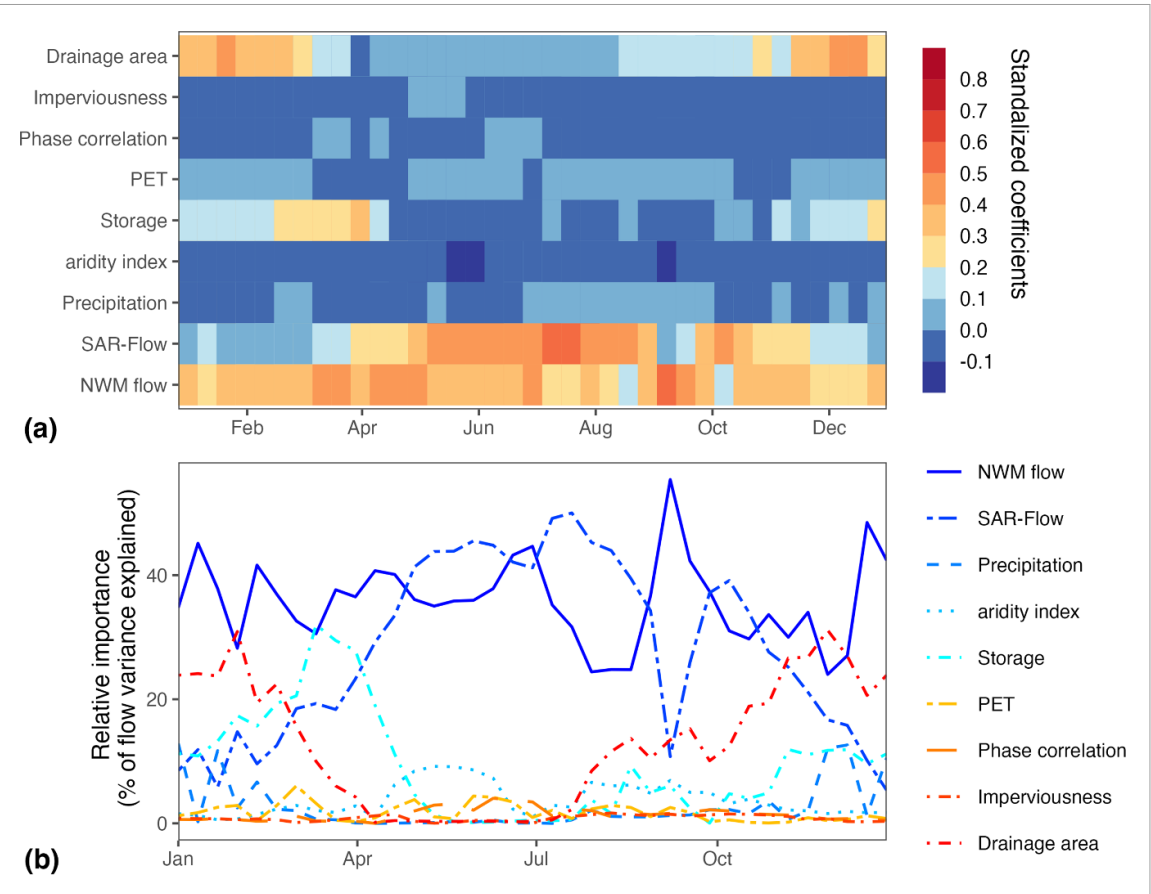


**Figure 5.** Role of various predictors in predicting ABF using the STHM-SAR model for the natural basins: (a) standardized model coefficients of selected predictor variables; (b) average relative importance, expressed as % variance explained by the hierarchical model, of the selected predictor variables.

provides the capability for continuous adjustments and updates to the forecast as new and relevant data becomes available (for example through the Next Generation Water Resource Modeling Framework (Odgen et al 2021, www.weather.gov/media/owp/oh/docs/2021-OWP-NWM-NextGen-Framework.pdf). This adaptability by developing improved estimates of antecedent conditions is crucial for maintaining the forecast's precision and relevance.

# 3.3. STHM-SAR predictors' contribution

The STHM-SAR model, incorporating all predictors from Fang *et al* (2024) along with the 3 day average streamflow estimated from GFDS-SAR estimates, resulted in improvements in 86% of sites from natural basins, and 76% of sites from coastal basins (figure 4(c)). To better understand the impact of individual predictors, each predictor was assessed using the relative importance estimator proposed by (Grömping 2007) (figure 5). The NWM streamflow alone accounts for more ~43% of the variance in predicting ABF across the CONUS proving the value of having an operational, process-based model to draw on. Critically, this suggests that the NWM prediction is doing well at capturing variation in flow regimes but not magnitudes. SAR-derived flow contributes

significantly as well, explaining 27% of the corresponding variance. The remaining predictors contribute between 5%–12% of the observed streamflow variance, as depicted in figure 5.

From figure 5(a), it is evident that, apart from the coefficients associated with SAR-flow and NWM, the coefficients of other predictors were predominantly negative. This indicates an inverse relationship between these predictors and the observed streamflow. According to figure 5(b), the impact of individual hydroclimatic predictors on regionalization performance is relatively limited. In contrast, combinations of these predictors play a more substantial role, especially during specific periods. Notably, the combination of PET and aridity index together explained over 10% of the streamflow variance. This underscores the importance of considering specific combinations of hydroclimatic information, RS data and NWM predictions, as they can substantially enhance the understanding and prediction of ABF conditions across CONUS.

In figure 5(b), it is evident that NWM reanalysis streamflow predominantly contributes to explaining the observed streamflow variance particularly accounting for 54% overall on average in warmer seasons. Notably, SAR-flow provides better antecedent

conditions, particularly when NWM experiences limited skill in predicting ABF in the summer and fall months. This demonstrates the synergy between these predictors, where SAR-flow fills in the gaps and enhances predictive accuracy, ensuring a more reliable estimation. Particularly, during the months of June and September, SAR-flow becomes especially influential, explaining over 35% of the streamflow variance.

# 4. Discussion

The proposed STHM-SAR framework used the same model structure as STHM (Fang et al 2024), but showing more local accuracy through improvements in antecedent conditions by replacing the previous drainage area based depth of streamflow with the SAR-derived flow at the HUC08 level. The results of our study confirm the effectiveness of the proposed framework in GAGES-II natural basins. The spatial calibration of the modeled streamflow, illustrated in figure 4, indicates that the validated STHM-SAR model can improve predictive accuracy. One of the notable strengths of the suggested approach lies in its simplicity; it does not require complex models or data assimilation techniques or additional predictors to enhance streamflow predictions and relies on open data and products. It leverages the inherent dynamics present in RS data to effectively improve antecedent conditions as illustrated in figure 5. This approach not only simplifies the post processing modeling process but also demonstrates the potential of utilizing existing data creatively to address challenges in ABF prediction, especially in regions lacking comprehensive streamflow measurements (figure 3).

The modeled ABF conditions, as depicted in figure 4 aligns closely with the magnitude of the observed streamflow, surpassing the performance of STHM flow from Fang *et al* (2024). This alignment underscores the utility of the proposed SAR-derived flow in better representing all locations across a diverse domain. This achievement is attributed to the integration of the correlation between the *M/C* ratio and observed flow from inundation information and leveraged using the PCR method. By utilizing the stage and *M/C* ratio dependencies, the SAR-derived flow not only captures the high streamflow patterns more effectively but demonstrates its capability in bridging the gap in data-scarce regions.

Compared with STHM (Fang et al 2024), the substantial improvement in the STHM-SAR performance stems from the addition of SAR-derived data. Satellite products provide valuable information about ANF conditions that can complement or substitute *in-situ* readings. The increasing availability of high-resolution earth observation data, offered freely by numerous space agencies, opens avenues for enhancing ANF forecasting and reanalysis based on Earth

Observation along with openly available physical modeling-based streamflow predictions.

## 5. Conclusions

The study demonstrates the effectiveness of integrating SAR data with the NWM to enhance predictions of ANF in ungauged basins. The spatial-temporal Hierarchical model for ANF prediction using STHM-SAR shows a significant improvement of 54% on average compared to previous STHM results (Fang et al 2024), particularly benefiting coastal regions. The spatio-temporal evaluation for natural basins results indicate promising performance, with SAR data contributing substantially to explaining variance by 27% on average.

The correlation analysis between SAR-derived and observed streamflow highlights the accuracy of SAR-derived streamflow as a proxy for ABF prediction, especially during high-flow events. The STHM-SAR model, incorporating SAR-derived streamflow, outperforms the raw NWM predictions, with 81.6% of sites showing improved skill. The spatial distribution of model-predicted high streamflow demonstrates significant enhancements, particularly in basins lacking gauged locations.

The analysis of predictors' contribution in the STHM-SAR model emphasizes the importance of NWM reanalysis streamflow and SAR-derived flow, which together explain a significant portion of observed streamflow variance. The study underscores the value of considering specific hydroclimatic factors and leveraging RS data to enhance flood prediction capabilities, especially in data-scarce regions and ungauged basins. Overall, the findings of this study highlight the potential of RS data integration with physical-based model streamflow predictions and suggest avenues for further research and improvements in flood prediction modeling, contributing to more effective risk management and response strategies.

# Data availability statement

Data Availability Statement: The GFDL data can be accessed at <a href="https://www.gdacs.org/flooddetection/DATA/SINGLE/SignalTiffs/">www.gdacs.org/flooddetection/DATA/SINGLE/SignalTiffs/</a>. The complete data workflow including data download on S Fang (2023) <a href="https://doi.org/10.5281/zenodo.7574439">https://doi.org/10.5281/zenodo.7574439</a> from Zenodo repository.

The data that support the findings of this study are openly available at the following URL/DOI: https://zenodo.org/records/7574439.

# Acknowledgment

We are grateful for the support from NSF Projects EAR-2208562, DMS-2152887, and CBET-2151651.

## **Conflict of interest**

The authors declare that they have no known competing financial interests or personal relationships that could have influenced the work reported in this paper.

#### **ORCID iDs**

Shiqi Fang **b** https://orcid.org/0000-0001-5872-996X

J Michael Johnson https://orcid.org/0000-0002-5288-8350

A Sankarasubramanian https://orcid.org/0000-0002-7668-1311

## References

- AghaKouchak A, Farahmand A, Melton F S, Teixeira J, Anderson M C, Wardlow B D and Hain C R 2015 Remote sensing of drought: progress, challenges and opportunities *Rev. Geophys.* 53 452–80
- Alquraish M M and Khadr M 2021 Remote-sensing-based streamflow forecasting using artificial neural network and support vector machine models *Remote Sens.* 13 4147
- Archfield S A *et al* 2015 Accelerating advances in continental domain hydrologic modeling *Water Resour. Res.* 51 10078–91
- Beck H E, de Jeu R A M, Schellekens J, van Dijk A and Bruijnzeel L A 2009 Improving curve number based storm runoff estimates using soil moisture proxies *IEEE J. Sel. Top. Appl. Earth Obs. Remote Sens.* 2 250–9
- Blodgett D, Johnson J M and Bock A 2023 Generating a reference flow network with improved connectivity to support durable data integration and reproducibility in the coterminous US *Environ. Modell. Software* 165 105726
- Browne M W 2000 Cross-validation methods *J. Math. Psychol.* 44 108–32
- Camps-Valls G and Bruzzone L 2005 Kernel-based methods for hyperspectral image classification *IEEE Trans. Geosci. Remote Sens.* 43 1351–62
- Clark M P, Fan Y, Lawrence D M, Adam J C, Bolster D, Gochis D J, Hooper R P, Kumar M, Leung L R and Mackay D S 2015 Improving the representation of hydrologic processes in Earth system models *Water Resour. Res.* 51 5929–56
- Cooper E S, Dance S L, Garcia-Pintado J, Nichols N K and Smith P J 2018 Observation impact, domain length and parameter estimation in data assimilation for flood forecasting *Environ. Modell. Software* **104** 199–214
- Falcone J A 2011 GAGES-II: Geospatial attributes of gages for evaluating streamflow *US Geological Survey* (available at: https://pubs.usgs.gov/publication/70046617)
- Fang S Q, Johnson J M, Yeghiazarian L and Sankarasubramanian A 2024 improved national-scale above-normal flow prediction for gauged and ungauged basins using a spatio-temporal hierarchical model Water Resour. Res. 60 20
- Feng D, Fang K and Shen C 2020 Enhancing streamflow forecast and extracting insights using long-short term memory networks with data integration at continental scales Water Resour. Res. 56 e2019WR026793
- Frame J M, Kratzert F, Raney A, Rahman M, Salas F R and Nearing G S 2021 Post-processing the national water model with long short-term memory networks for streamflow predictions and model diagnostics JAWRA J. Am. Water Resour. Assoc. 57 885–905
- Ghotbi S, Wang D, Singh A, Mayo T and Sivapalan M 2020 Climate and landscape controls of regional patterns of flow duration curves across the continental united states: statistical approach *Water Resour. Res.* 56 e2020WR028041

- Gleason C J, Smith L C and Lee J 2014 Retrieval of river discharge solely from satellite imagery and at-many-stations hydraulic geometry: sensitivity to river form and optimization parameters *Water Resour. Res.* **50** 9604–19
- Grömping U 2007 Estimators of relative importance in linear regression based on variance decomposition *Am. Stat.* **61** 139–47
- Hong Y and Adler R F 2008 Estimation of global SCS curve numbers using satellite remote sensing and geospatial data *Int. J. Remote Sens.* 29 471–7
- Hostache R, Chini M, Giustarini L, Neal J, Kavetski D, Wood M, Corato G, Pelich R-M and Matgen P 2018 Near-real-time assimilation of SAR-derived flood maps for improving flood forecasts *Water Resour. Res.* 54 5516–35
- Johnson F, White C J, van Dijk A, Ekstrom M, Evans J P, Jakob D, Kiem A S, Leonard M, Rouillard A and Westra S 2016 Natural hazards in Australia: floods *Clim. Change* 139 21–35
- Johnson J M, Fang S, Sankarasubramanian A, Rad A M, Kindl da Cunha L, Jennings K S, Clarke K C, Mazrooei A and Yeghiazarian L 2023 Comprehensive analysis of the NOAA National Water Model: a call for heterogeneous formulations and diagnostic model selection *J. Geophys. Res.* Atmos. 128 e2023JD038534
- Johnson J M, Munasinghe D, Eyelade D and Cohen S 2019 An integrated evaluation of the National Water Model (NWM)–Height Above Nearest Drainage (HAND) flood mapping methodology Nat. Hazards Earth Syst. Sci. 19 2405–20
- Kratzert F, Klotz D, Shalev G, Klambauer G, Hochreiter S and Nearing G 2019 Towards learning universal, regional, and local hydrological behaviors via machine learning applied to large-sample datasets *Hydrol. Earth Syst. Sci.* 23 5089–110
- Kugler Z and De Groeve T 2007 *The Global Flood Detection System* (Office for Official Publications of the European Communities) p 45
- Maidment D R 2009 FEMA flood map accuracy pp 1–10
  Martinis S, Twele A and Voigt S 2009 Towards operational near
  real-time flood detection using a split-based automatic
  thresholding procedure on high resolution TerraSAR-X data
  Nat. Hazards Earth Syst. Sci. 9 303–14
- Mazrooei A and Sankarasubramanian A 2019 Improving monthly streamflow forecasts through assimilation of observed streamflow for rainfall-dominated basins across the CONUS J. Hydrol. 575 704–15
- Mazrooei A, Sankarasubramanian A and Wood A W 2021 Potential in improving monthly streamflow forecasting through variational assimilation of observed streamflow *J. Hydrol.* **600** 126559
- McCuen R H, Knight Z and Cutter A G 2006 Evaluation of the Nash–Sutcliffe efficiency index J. Hydrol. Eng. 11 597–602
- McKay L, Bondelid T, Dewald T, Johnston J, Moore R and Rea A 2012 NHDPlus Version 2: User Guide (US Environmental Protection Agency) p 745
- Moriasi D N *et al* 2007 Model evaluation guidelines for systematic quantification of accuracy in watershed simulations *Trans*. *ASABE* **50** 885–900 (available at: https://elibrary.asabe.org/abstract.asp?aid=23153)
- National Research Council 2006 Toward a New Advanced

  Hydrologic Prediction Service (AHPS National Academies

  Press)
- National Weather Service 2022 National Weather Service (Office of Water Prediction)
- Ogden F, Avant B, Bartel R, Blodgett D, Clark E and Cosgrove B 2021 The next generation water resources modeling framework: open source, standards based, community accessible, model interoperability for large scale water prediction AGU Fall Meeting Abstracts vol 2021 p H43D-01 (available at: https://ui.adsabs.harvard.edu/abs/2021AGUFM.H43D)
- Revilla-Romero B, Wanders N, Burek P, Salamon P and de Roo A 2016 Integrating remotely sensed surface water extent into continental scale hydrology *J. Hydrol.* **543** 659–70

- Sahoo D P, Sahoo B, Tiwari M K and Behera G K 2022 Integrated remote sensing and machine learning tools for estimating ecological flow regimes in tropical river reaches J. Environ. Manage. 322 116121
- Salas J, Saha A and Ravela S 2023 Learning inter-annual flood loss risk models from historical flood insurance claims *J. Environ. Manage.* 347 118862
- Seager R and Ting M 2017 Decadal drought variability over North America: mechanisms and predictability Curr. Clim. Change Rep. 3 141–9
- Sogno P, Klein I and Kuenzer C 2022 Remote sensing of surface water dynamics in the context of global change—a review *Remote Sens.* 14 2475
- Sperna Weiland F, Van Beek L, Kwadijk J and Bierkens M 2012 Global patterns of change in discharge regimes for 2100 *Hydrol. Earth Syst. Sci.* 16 1047–62
- Tarpanelli A, Santi E, Tourian M J, Filippucci P, Amarnath G and Brocca L 2019 Daily river discharge estimates by merging satellite optical sensors and radar altimetry through artificial neural network *IEEE Trans. Geosci. Remote Sens.* 57, 329–41
- Tayal K, Renganathan A and Lu D 2024 Improving streamflow predictions across CONUS by integrating advanced machine learning models and diverse data *Environ. Res. Lett.* 19 104009
- Tsokas A, Rysz M, Pardalos P M and Dipple K 2022 SAR data applications in earth observation: an overview *Expert Syst. Appl.* **205** 117342

- Van Dijk A I J M, Brakenridge G R, Kettner A J, Beck H E, De Groeve T and Schellekens J 2016 River gauging at global scale using optical and passive microwave remote sensing *Water Resour. Res.* 52 6404–18
- Van Dijk S, Molloy P, Varinli H, Morrison J and Muhlhausler B 2015 Epigenetics and human obesity *Int. J. Obesity* **39** 85–97
- Vinukollu R K, Wood E F, Ferguson C R and Fisher J B 2011 Global estimates of evapotranspiration for climate studies using multi-sensor remote sensing data: evaluation of three process-based approaches *Remote Sens. Environ.* 115 801–23
- Viterbo F, Mahoney K, Read L, Salas F, Bates B, Elliott J, Cosgrove B, Dugger A, Gochis D and Cifelli R 2020 A multiscale, hydrometeorological forecast evaluation of national water model forecasts of the May 2018 Ellicott City, Maryland, Flood *I. Hydrometeorl.* 21 475–99
- Wood E F, Roundy J K, Troy T J, Van Beek L, Bierkens M F, Blyth E, de Roo A, Döll P, Ek M and Famiglietti J 2011 Hyperresolution global land surface modeling: meeting a grand challenge for monitoring Earth's terrestrial water *Water Resour. Res.* 47 W05301
- Xu N, Zheng H, Ma Y, Yang J, Liu X and Wang X 2021 Global estimation and assessment of monthly lake/reservoir water level changes using ICESat-2 ATL13 products Remote Sens. 13 2744
- Yoon H N, Marshall L, Sharma A and Kim S 2022 Bayesian model calibration using surrogate streamflow in ungauged catchments *Water Resour. Res.* 58 e2021WR031287